Eur. Phys. J. D **35**, 97–104 (2005)
DOI: 10.1140/epjd/e2005-00227-1

THE EUROPEAN PHYSICAL JOURNAL D

Relevance of sub-surface chip layers for the lifetime of magnetically trapped atoms

B. Zhang[1], C. Henkel[1], E. Haller[2], S. Wildermuth[2], S. Hofferberth[2], P. Krüger[2], and J. Schmiedmayer[2,a]

[1] Institut für Physik, Universität Potsdam, Am Neuen Palais 10, 14469 Potsdam, Germany
[2] Physikalisches Institut, Universität Heidelberg, Philosophenweg 12, 69120 Heidelberg, Germany

Received 23 March 2005 / Received in final form 21 June 2005
Published online 17 August 2005 –

Abstract. We investigate the lifetime of magnetically trapped atoms above a planar, layered atom chip structure. Numerical calculations of the thermal magnetic noise spectrum are performed, based on the exact magnetic Green function and multi layer reflection coefficients. We have performed lifetime measurements where the center of a side guide trap is laterally shifted with respect to the current carrying wire using additional bias fields. Comparing the experiment to theory, we find a fair agreement and demonstrate that for a chip whose topmost layer is metallic, the magnetic noise depends essentially on the thickness of that layer, as long as the layers below have a much smaller conductivity; essentially the same magnetic noise would be obtained with a metallic membrane suspended in vacuum. Based on our theory we give general scaling laws of how to reduce the effect of surface magnetic noise on the trapped atoms.

PACS. 32.80.Pj Optical cooling of atoms; trapping – 03.75.Be Atom and neutron optics

1 Introduction

In the field of atom cooling and trapping, there has been rapid progress towards miniaturisation and integration (for a general overview see [1,2]), as the present special issue illustrates. Small particle traps are now being implemented as the building blocks of future quantum computers [3,4]. Integrated atom optical circuits also distribute coherent matter waves for interferometric [5] and nano lithographic applications.

Recent experiments are working with hybrid electromagnetic solid-state surface guides, or "atom chips", where trapping and cooling of atoms to μK temperatures and down to the Bose-Einstein degeneracy has been demonstrated [2,6–10]. It has become clear that such cold atoms are perturbed by thermal electromagnetic fields generated by the nearby, "hot" solid substrate, leading to heating, trap loss and scattering [11–13]. In previous work, one of the present authors (C.H.) and co-workers have derived the loss rate for a trapped atom that is coupled to fluctuating fields in the vicinity of a room-temperature metallic and/or dielectric surface (half-space structure) [14]. Actual experiments, however, use more complex chip structures involving several layers with lateral patterning. We focus here on the impact of the subsurface layers on atom trap lifetimes and compare the theory to experiments. On the theoretical side, numerical calculations have been set-up, building on the exact method of reference [14]. We consider loss processes that are due to a transition to an untrapped internal state (Zeeman sublevel). Experimentally, we have worked with a standard Z-wire trap [29] and added a magnetic bias field to shift the trap center with respect to the current carrying wire. This permits to differentiate between current fluctuations of technical origin and intrinsic thermal noise from the chip surface. The data are fairly well described by a theory without adjustable parameters. The calculations show that for chips whose top layer is a good metallic conductor, the resistivity and thickness of this layer are the essential parameters determining the magnetic noise and hence the trap lifetime. As long as they have a much larger resistivity, the subsurface layers do not actually play a role.

The paper is organized as follows: in Section 2, we review the theory for the loss rate and lifetime of an atom with a magnetic moment above a layered chip. The relevant loss rate is proportional to the magnetic field fluctuation spectrum. This we compute at thermodynamic equilibrium for the field, using the fluctuation-dissipation theorem and electromagnetic reflection coefficients for a multilayer chip. Section 3 describes the experimental procedures for the lifetime measurements and gives a detailed comparison between theory and experiment regarding atom trap lifetimes in miniaturized structures. Section 4 reviews scaling laws for both trap confinement

[a] e-mail: Joerg.Schmiedmayer@physik.uni-heidelberg.de

and lifetime and discusses optimization strategies. The final Section 5 gives a summary and outlook.

2 Internal spin flips

Neutral particles can be trapped in potentials created by electromagnetic fields that typically depend on their internal state (electronic, hyperfine or magnetic). We focus here on magnetic traps described by the Zeeman interaction

$$V_Z(\boldsymbol{r},t) = -\boldsymbol{\mu}\cdot\boldsymbol{B}(\boldsymbol{r},t), \tag{1}$$

where $\boldsymbol{\mu}$ is the particle's magnetic moment and $\boldsymbol{r}$ its (center of mass) position. A static field with a minimum of $|\boldsymbol{B}(\boldsymbol{r})|$ provides a trap for a subset of magnetic states, the weak field seekers: their magnetic moment is aligned antiparallel to the field. Many atom chip traps are based on this principle.

A loss process occurs when a fluctuating field induces a transition $|i\rangle \rightarrow |f\rangle$ of the particle to a state with a magnetic moment parallel to the field. The magnetic potential then has the opposite sign, and we can assume that the particle is rapidly expelled from the trap. These spin flips are described also by the interaction Hamiltonian (1), and are induced by fields with a frequency around the Bohr transition frequency $\omega_{fi} = (E_f - E_i)/\hbar$. A calculation based on Fermi's Golden Rule yields for the transition rate

$$\Gamma_{i\rightarrow f}(\boldsymbol{r}) = \sum_{\alpha\beta} \frac{\langle i|\mu_\alpha|f\rangle\langle f|\mu_\beta|i\rangle}{\hbar^2} S_B^{\alpha\beta}(\boldsymbol{r};-\omega_{fi}) \tag{2}$$

where $S_B^{\alpha\beta}$ is the magnetic field fluctuation spectrum evaluated at the transition frequency

$$S_B^{\alpha\beta}(\boldsymbol{r},\omega) = \int_{-\infty}^{+\infty} \mathrm{d}\tau\ \langle B_\alpha(\boldsymbol{r},t+\tau)B_\beta(\boldsymbol{r},t)\rangle e^{i\omega\tau}. \tag{3}$$

The spectrum is taken at the trap center $\boldsymbol{r}$, assuming that the spatial extension of the trap is sufficiently small. From these expressions, we can get the trap lifetime $1/\Gamma_{i\rightarrow f}$. We evaluate the atom's internal matrix elements $\langle i|\mu_\alpha|f\rangle$ as described in reference [14]. The magnetic field fluctuation spectrum $S_B^{\alpha\beta}(\boldsymbol{r},\omega)$ can be found with Green's function techniques as summarized in the following.

2.1 Magnetic field correlations

As discussed in reference [14], the spectral density of the magnetic field fluctuations is proportional to the imaginary part of the field's Green function $H_{ij}(\boldsymbol{r},\boldsymbol{r};\omega)$, according to the fluctuation-dissipation theorem. This approach is exact for a field in thermodynamic equilibrium, and it can be extended to non-equilibrium situations like a heated surface, possibly with temperature gradients. In that broader context, one can use a method that consists of incoherently adding the fields radiated by thermally excited currents in each volume element of the surface [15–17]. The boundary conditions at the vacuum interface and the damping inside the material have to be taken into account, however. Otherwise one gets a different numerical prefactor for some components of the noise spectrum S_B^{ij} or even a different power law as a function of distance. More details are discussed in the paper [18] in this issue.

Recall that the Green function describes the magnetic field radiated by a point magnetic moment. This field is the sum of the magnetic field in free space plus the field reflected from the surface. The free space field leads to a term $H_{ij}^{vac}(\boldsymbol{r},\boldsymbol{r};\omega)$ in the Green function that is actually independent of the trap position $\boldsymbol{r}$ and gives the spectral density of the blackbody field:

$$S_B^{(vac)ij}(\boldsymbol{r};\omega) = S_B^{(vac)}(\omega)\delta_{ij} \tag{4}$$

$$S_B^{(vac)} = \frac{\hbar\mu_0\omega^3}{3\pi c^3(1-e^{-\hbar\omega/k_BT})} \tag{5}$$

where T is the temperature of the surface and k_B the Boltzmann constant.

To calculate the field reflected from the surface, we expand the free-space magnetic field in plane waves and apply the reflection coefficients $r_{s,p}(u)$ for each wave incident on the surface. Here, s and p label the two transverse field polarizations and u is the sine of the angle of incidence. The corresponding spectral density depends only on the distance z to the surface and may be written in terms of a dimensionless tensor $h_{ij}(kz)$ [19]

$$S_B^{(ref)ij}(\boldsymbol{r},\omega) = S_B^{(vac)}(\omega)h_{ij}(kz), \tag{6}$$

where $k \equiv \omega/c$. h_{ij} is diagonal with elements $h_{xx} = h_{yy} = h_\parallel$ and $h_{zz} = h_\perp$ given by

$$h_\parallel(kz) = \frac{3}{4}\mathrm{Re}\int_0^{+\infty} \frac{u\mathrm{d}u}{\sqrt{1-u^2}} e^{2ikz\sqrt{1-u^2}} \times(r_p(u) + (u^2-1)r_s(u)) \tag{7}$$

$$h_\perp(kz) = \frac{3}{2}\mathrm{Re}\int_0^{+\infty} \frac{u^3\mathrm{d}u}{\sqrt{1-u^2}} e^{2ikz\sqrt{1-u^2}} r_s(u). \tag{8}$$

The range $u > 1$ corresponds to the evanescent part of the angular spectrum a magnetic dipole generates in free space. The square roots occurring in equations (7, 8) are chosen with positive imaginary part.

Note that for a half-space structure, the reflection coefficients are given by the Fresnel formulas at the surface; this has been used in previous work [14]. For a layered chip, r_λ ($\lambda = s,p$) are the effective reflection amplitudes from the multilayer structure, as illustrated in Figure 1. At the lowest interface ($n = 3$), the Fresnel reflection coefficients apply and are given by

$$r'_{s,n} = \frac{\sqrt{\varepsilon_n - u^2} - \sqrt{\varepsilon_{n+1} - u^2}}{\sqrt{\varepsilon_n - u^2} + \sqrt{\varepsilon_{n+1} - u^2}} \tag{9}$$

$$r'_{p,n} = \frac{\varepsilon_{n+1}\sqrt{\varepsilon_n - u^2} - \varepsilon_n\sqrt{\varepsilon_{n+1} - u^2}}{\varepsilon_{n+1}\sqrt{\varepsilon_n - u^2} + \varepsilon_n\sqrt{\varepsilon_{n+1} - u^2}} \tag{10}$$

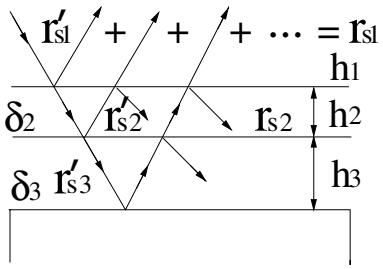

Fig. 1. A chip with two layers on top of a semi-infinite substrate. h_n is the thickness of the nth layer, δ_n denotes the optical path length for a single down and up ray in the nth layer. $r'_{\lambda n}$ are the Fresnel reflection coefficients at the interface between the layers no. n and $n+1$ ($\lambda = s, p$), while $r_{\lambda n}$ are the effective (multilayer) reflection coefficients from layer no. n.

where ε_n is the permittivity of the nth layer. The effective reflection coefficient off the nth layer is [20]

$$r_{\lambda,n} = \frac{r'_{\lambda,n} + r_{\lambda,n+1} e^{i\delta_{n+1}}}{1 + r'_{\lambda,n} r_{\lambda,n+1} e^{i\delta_{n+1}}} \tag{11}$$

where $r'_{\lambda,n}$ is the Fresnel coefficient (Eq. (9) or (10)) and $r_{\lambda,n+1}$ the amplitude for the layer structure below; δ_n is the phase shift in the layer:

$$\delta_n = 2h_n k \sqrt{\varepsilon_n - u^2}, \tag{12}$$

h_n is the layer thickness and the square root is chosen with positive imaginary part. In the case of Figure 1, the lowest layer is $n = 3$ and we put $r_{\lambda,3} \equiv r'_{\lambda,3}$. We then apply equation (11) recursively for the next layers, until the reflection from the topmost layer, $r_{\lambda,1} = r_{\lambda,1}(u)$, is found. This is the coefficient we use in equations (7, 8). The integral over u is computed numerically, with care being taken for the (integrable) singularity $1/\sqrt{1-u^2}$ at the point $u = 1$.

2.2 Impact of subsurface layers

Based on Section 2.1, we calculate the loss rate for a trapped rubidium atom from equation (2) and then get the lifetime $1/\Gamma_{i\to f}$. A comparison to experimental data can be found in Section 3.4 (see Fig. 7). We discuss here the relevance of the subsurface layers on the lifetime.

We plot in Figure 2 the trap lifetime above a gold layer deposited on a substrate with varying resistivity ϱ_3 normalized to a gold layer suspended in vacuum ($\varrho_3 = \infty$). The subsurface layer hardly has an impact on the trap lifetime, as long as the topmost layer has a resistance that is smaller by at least two orders of magnitude. We now give an analytical argument to understand this more clearly. As mentioned in previous work [14], the integrands in equations (7, 8), as functions of u are peaked around $u \sim u_{max}$. This is because the exponential $e^{2ikz\sqrt{1-u^2}} \approx e^{-2kzu}$ decreases only when $u \sim 1/(kz) \gg 1$. On the other hand, the other factors in the integrands increase as powers of u. The value of the integral is thus dominated by values

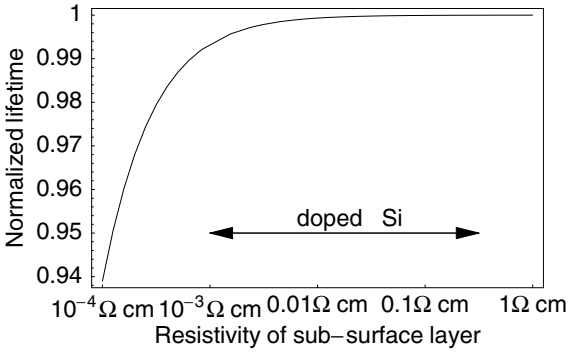

Fig. 2. Trap lifetime vs. resistivity of sub-surface layer, normalized to a single layer suspended in vacuum (gold, 3.1 μm thick, resistivity 2.2 $\mu\Omega$ cm). The distance from the trapped atom to the top surface is 10 μm. The layer permittivities are $\varepsilon_0\varepsilon_n = \varepsilon_0 + i/(\omega\varrho_n)$ and $\omega/2\pi = 1.1$ MHz.

$u \sim u_{max}$ around the maximum $u_{max} \gg 1$, and it is accurate to use the asymptotic expansion of the reflection coefficients equations (9–11) for large $u \gg 1$. Let us focus on a distance comparable to the skin depth in the gold layer (subscript 2) at the transition frequency, and a sub-surface layer with a much smaller conductivity. We check that the maximum then occurs around $u_{max}^2 \sim |\varepsilon_2| \gg |\varepsilon_3| \gg 1$. If we consider the first order expansion in this regime, we get

$$r_{s,1} = \frac{(1-\Delta_s^2)(1-e^{i\delta_2})}{(1-\Delta_s)^2 - (1+\Delta_s)^2 e^{i\delta_2}}, \tag{13}$$

with

$$\Delta_s = i\sqrt{\varepsilon_2 - u^2}/u. \tag{14}$$

And

$$r_{p,1} = -1 + \Delta_p \frac{1+e^{i\delta_2}}{1-e^{i\delta_2}}, \tag{15}$$

where

$$\Delta_p = 2i\sqrt{\varepsilon_2 - u^2}/(\varepsilon_2 u). \tag{16}$$

Note that $|\Delta_p| \ll 1$ around u_{max}, while $|\Delta_s| \sim 1$. From the equations above, we see that ε_3 has cancelled from the multilayer coefficients. This means that the sub-surface layer has no effect on the trap lifetime as long as its resistance is larger than the topmost (metallic) layer and the trap is at a distance comparable to the skin depth in the metal or smaller.

In Figure 3, we plot the lifetime (normalized to the lifetime above a gold half-space) for varying thickness t of the topmost layer. The black solid line is the asymptotic result obtained by inserting equations (13, 15) into the integrals for the Green functions. The triangles and squares mark calculations for a gold/silicon and gold/vacuum structure, using the full multilayer reflection coefficients (11). We see that the three situations give the same trap lifetime. For these chip parameters, reducing the gold layer thickness thus improves the trapping conditions. This happens because the layer being much thinner than the skin depth at the relevant frequency ($\xi \equiv (2\varrho/(\mu_0\omega))^{1/2}$), it is a thermal radiation source across its whole thickness. For this

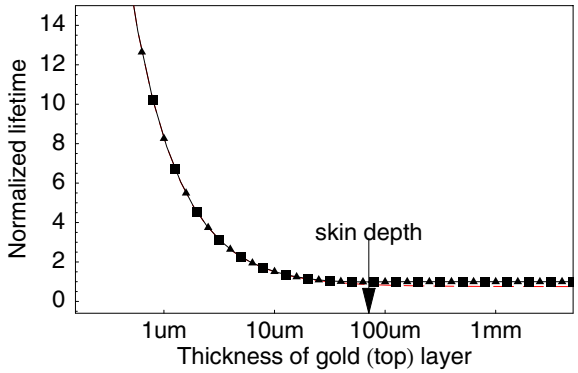

Fig. 3. Trap lifetime vs. thickness t of the top layer (gold), normalized to a gold half-space; distance of trapped atom to the surface: $z = 10\,\mu$m. Black solid line: based on the asymptotic expansion (13, 15) of the reflection coefficients in the magnetic Green tensor. Triangles: gold/silicon structure; boxes: gold layer in vacuum. For these two, the full multilayer reflection coefficients are used. Dashed (red) line: prediction $(t+z)/t$ of the quasistatic theory, valid when t is much smaller than the skin depth. The arrow marks the skin depth in gold at the transition frequency 1.1 MHz. The layer resistivities are given in Figure 7.

reason, the quasi-static approximation introduced in reference [17] gives an excellent agreement with the exact calculation, as illustrated by the dashed (red) curve in the figure. This also applies to the layer theory plotted in Figure 7. Only when the layer thickness exceeds the skin depth, $t \gg \xi$, a difference appears which is due to skin effect corrections that start to play even though the distance $z \sim 0.1\,\xi$ here. The impact of the skin depth is also visible in Figure 7 (dashed line) from the crossover above a semi-infinite gold chip: at distances $z \gg \xi$, the lifetime increases faster with distance (see Ref. [14]) and ultimately approaches the value given by the blackbody radiation spectrum (5) (beyond the figure range).

We have observed that at a much larger distance (beyond the skin depth), the lifetime shows a minimum if the gold layer is slightly thinner than the skin depth (barely visible in Fig. 3). A similar behaviour has been noted recently as a function of skin depth above cylindrical and planar structures [11]. This is related to an absorption resonance in the reflection from a thin metallic layer, as discussed for example in reference [22]. Above the planar structure considered here, we do not expect this effect to be measurable since the surface-induced loss rate already becomes too small for $z \gg \xi$.

3 Experiment

Over the last three years, the reduction of lifetimes in traps close to conducting surfaces has been investigated in a number of experiments. Both the influence of technical noise [23] and thermal noise near bulk conductors of different materials [12,24,25] have been found to be in quantitative agreement with the theory presented above. Layered structures, which promise to reduce loss rates due to thermal currents, have only been explored in an experiment by the Vuletic group [21] which investigated the loss above a 2 μm thick and 10 μm wide Cu wire and a Si substrate. The Hinds group recently reported measurements above a permanently magnetized structured covered by a thin (400 nm) gold layer [10]. Here we present a configuration that allows to investigate the loss due to spin flips over a thin metal layer in a configuration where the contributions of technical noise can be kept constant and the thermal noise sources can be studied over a wide range of distances near a multilayer structure.

3.1 Experimental set-up

The experiments were performed with our standard atom chip set-up in Heidelberg [27,33]. We start with more than 10^8 ^{87}Rb atoms accumulated in a mirror magneto-optical trap (MOT) a few mm from the chip surface. The atoms are subsequently transferred to a purely magnetic Z-wire trap and cooled to $\sim$10 μK by radio frequency (RF) evaporation. Both the MOT and the magnetic trap are based on copper wire structures mounted directly underneath the chip [27]. The resulting sample of $>10^6$ atoms is then loaded to the selected chip trap, where a second stage of RF evaporative cooling creates either a BEC or thermal cloud just above the critical condensation temperature.

In order to determine the cloud's distance from the surface z we image the atomic cloud near the surface in situ by resonant absorption imaging with a $\sim$3.5 μm resolution. The imaging light path is slightly inclined ($\sim$25 mrad) with respect to the chip mirror surface. For distances 300 μm $> z >$ 5 μm, this leads to a duplicated absorption image [9] which allows a direct measurement of the height (see Fig. 4).

While the wire currents are very well known, the strength of the external bias fields has to be calibrated by measuring z at sufficiently large heights (Fig. 4). Diffraction effects from the chip surface and our imaging resolution do not allow to measure z for very close ($z < 5\,\mu$m) surface approaches. In these cases, we use the calibrated values of the bias fields together with the measured wire currents to infer z from numerical calculations of the trapping potential, leading to an accuracy better than 1 μm. These calculations include the actual arrangement of the wires on the chip [28].

3.2 Atom chip set-up

Our atom chip set-up incorporates various different layers (see Fig. 5). The atom chip itself was fabricated using our standard method [26]. It is grown on a 700 μm thick silicon substrate covered with an insulation layer of SiO_2 (500 nm) and a Ti adhesion layer (35 nm). The gold layers with the desired wire patterns are created using a nanolithographic lift-off technique adapted for thick ($>1\,\mu$m) layers. The major chip area used in this experiment is covered with a 1.8 μm thick reflection layer containing gaps (width 10 μm) to isolate the current carrying wires.

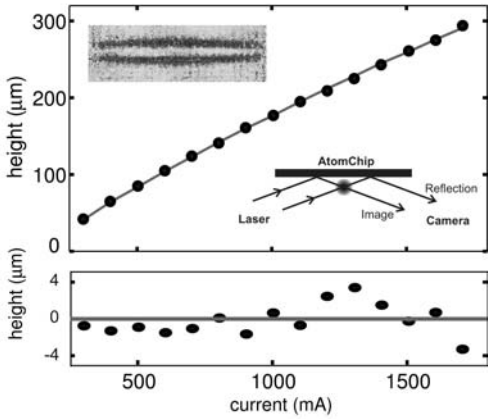

Fig. 4. Example of the calibration of the magnetic bias field. Top: measured height vs. current in Z-wire at a bias field of 12 G. The line represents a calculation using a model of the actual wire configuration with the bias field as a free parameter. Once the bias field is known it can be used to calculate other heights at positions closer to the chip. Bottom: residuals for the fit. Inset: the imaging laser is reflected of the chip surface which results in two images of the atom cloud. The upper inset shows an absorption image of a trapped atom cloud ∼35 μm away from the atom chip surface and the lower inset shows an exaggerated scheme of the set-up.

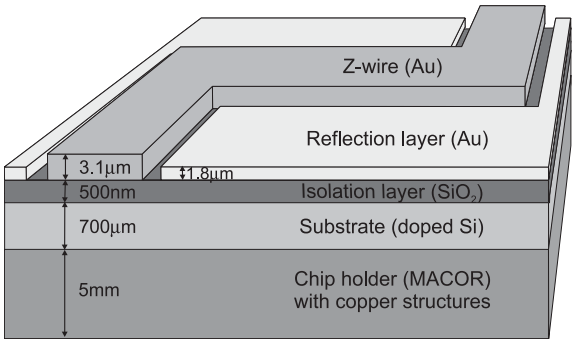

Fig. 5. Layer structure of the chip. The resistivities of the layers are $\varrho > 10^6\ \Omega\,\mathrm{cm}$ (MACOR), $\varrho = 1.7\ \mu\Omega\,\mathrm{cm}$ (copper), $\varrho = 17\ \mathrm{m}\Omega\,\mathrm{cm}$ (doped silicon), $\varrho > 10^4\ \Omega\,\mathrm{cm}$ (SiO_2) and $\varrho = 2.2\ \mu\Omega\,\mathrm{cm}$ (gold).

The thicker Z-wire structures were fabricated with a two layer technique allowing a thickness of 3.1 μm (wire cross-section $3.1 \times 100\,\mu\mathrm{m}^2$). The atom chip structure is placed on top of a 5 mm thick ceramics chip holder (MACOR).

3.3 Lifetime measurements

The lifetimes of trapped ultra cold ^{87}Rb atoms were measured in a Ioffe-Pritchard type microtrap generated by currents flowing through the Z-shaped wire. The measurements are done with $\sim 1 \times 10^5$ thermal atoms at $\sim 1\,\mu$K in a trap created with a current of 2 A and a Larmor frequency of $\omega_{fi}/2\pi = 1.1$ MHz at the trap minimum (corresponding to a field of 1.5 G).

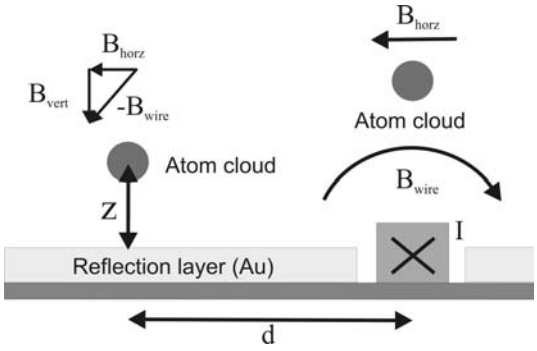

Fig. 6. Lateral trap displacement. An external horizontal magnetic field $\boldsymbol{B}_{horz}$ cancels the circular magnetic field $\boldsymbol{B}_{wire}$ of a current carrying wire directly over the wire. By applying an additional vertical field $\boldsymbol{B}_{vert}$ perpendicular to the chip surface, the trap can be positioned at a distance d from the wire and a height z above the chip surface.

The microtraps on the chip are created in the side guide configuration [1]. In the standard configuration the magnetic field $\boldsymbol{B}_{wire}$ of the the Z-shaped wire is (nearly) canceled directly above the center of the Z wire by a horizontal field $\boldsymbol{B}_{horz}$ (see Fig. 6). By adding a vertical magnetic field component $\boldsymbol{B}_{vert}$ the bias field is rotated around the central wire of the Z and with it the trap minimum. By adjusting the strength and orientation of the bias field the trap minimum can be positioned at a given distance d from the current carrying wire and at an given height z above the 1.8 μm thick gold layer of the chip (Fig. 6).

Placing the trap a significant distance away from the Z-wire allows us to keep the trap parameters nearly constant for each height above the surface. The further away one moves, the easier it is to keep the traps equal, independent of the height for the same wire current. But the traps get shallower at larger distance from the trapping wire. A shallow trap cannot be brought close to the surface for the lifetime measurements, because the trap depth is reduced due to the atom-surface interaction potential. Atoms are thus lost by evaporation across the potential barrier towards the chip surface. This leads to a significant cooling of the sample: in a dense cloud, evaporation leads typically to a final temperature of about 1/10th of the trap depth.

For each lifetime measurement we image either in situ or after a time-of-flight expansion. The former allows measurements down to lower atom number, the latter allows us to determine both the number of atoms and the temperature of the atoms. Both measurements of atom number agree, and both are used to determine the lifetime of the trapped clouds.

The independent measurement of the temperature is crucial because it permits to see if we have additional losses due to surface induced evaporation. A decrease in temperature is a direct indication that in addition to spin flips, atoms cross the lowered potential barrier towards the surface, resulting in a reduction of the lifetime. We observe that the decay of the atom number is then generally non-exponential. The height at which this becomes

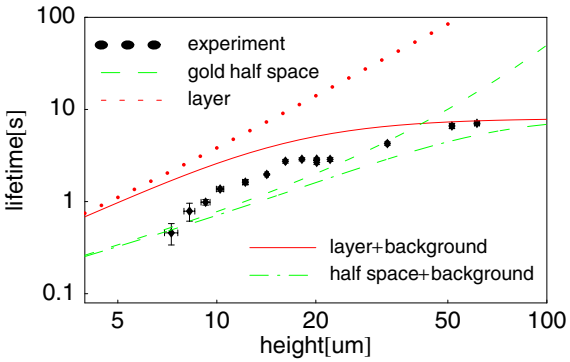

Fig. 7. Experimental data and theoretical predictions for the trap lifetime in a miniaturized magnetic Ioffe-Pritchard type trap. Symbols: life time data for a trap laterally displaced by 280 μm with respect to the current-carrying wire structure. Below 10 μm distance, surface evaporation decreases the lifetime. Lines: theoretical predictions with different level of detail for loss processes (spin flips) induced by thermal surface noise. The atom transits from $|F_i, m_i\rangle = |2, 2\rangle$ to $|F_f, m_f\rangle = |2, 1\rangle$, the transition (Larmor) frequency being $\omega_{fi}/2\pi = 1.1$ MHz. Dots (red line): layered chip (thin gold layer, doped silicon substrate, see parameters in Fig. 5). Solid (red) line: layered chip structure, including the measured trap lifetime at large distance. Dashed (green) line: bulk substrate (gold half-space). Dot-dashed (green) line: bulk structure, including the large distance trap lifetime.

important varies from $z = 3\,\mu$m for moderately confining traps directly over the wire up to $z = 40\,\mu$m for very shallow traps at a lateral distance $d = 520\,\mu$m from the trapping wire.

In the following comparison between calculation and experiment we only consider data where the temperature stays constant so that the main loss mechanicms are surface-induced spin flips and background collisions.

3.4 Comparison theory–experiment

To investigate the influence of the thermal noise we choose a distance $d = 280\,\mu$m as a compromise between being dominated by technical noise for small d and losing atoms due to evaporation towards the surface at large d.

In order to make a comparison between theory and experiment, we plot in Figure 7 both experimental data (symbols) and numerical calculations (lines). A agreement to better than a factor of two is found down to distances of a few microns when the theory takes into account (i) the finite thickness of the topmost (gold) layer and (ii) a distance-independent loss rate (red line). We stress that the latter rate is taken from the experimental data (saturation at large distance) so that the theory has no adjustable parameters. The figure shows that the lifetime above a thin (few μm thick) gold layer is significantly enhanced compared to a gold half space. We have checked that adding a MACOR or copper substrate below the thick silicon wafer does not change the results of the calculation. We attribute the discrepancy between experiment and theory to technical noise in wire current and bias field, and to atom-surface potentials that lower the potential barrier towards the surface, as also suggested by the Vuletic group [21]. As mentioned above, this mechanism becomes more important at short distance (below a few micron).

4 Optimization strategies for trap loss

We now discuss briefly strategies to reduce trap loss by optimizing different chip parameters. We focus on a flat, rectangular wire (thickness $t \ll$ width w) and on a trap with a specific transverse confinement given by a fixed magnetic field gradient $\mathrm{d}B/\mathrm{d}z$. The distance to the chip z can be adjusted with additional bias fields and is kept as a free parameter. The magnetic gradient above the center of the rectangular wire is given by [2,31,33]

$$\frac{\mathrm{d}B}{\mathrm{d}z} \approx \frac{\mu_0}{4\pi}\frac{8I}{w^2+4z^2} = \frac{\mu_0}{4\pi}\frac{8jtw}{w^2+4z^2} \tag{17}$$

where j is the current density (assumed to be uniform across the wire area). The maximum confinement is theoretically achieved at the surface $z = 0$, in practice reasonably large values occur in the range $z \leq w$. A strong confinement also requires a large current density, but this leads to a significant ohmic dissipation in the wire and an increase in temperature, as studied by Groth et al. [26]. Let us assume a linear temperature dependence of the resistance, $\varrho(T) = \varrho_0 + \alpha T$ where αT is the contribution of scattering by phonons and ϱ_0 is the zero temperature resistivity related to the scattering by impurities [32]. The temperature increase can then be written in the form

$$\begin{aligned}\Delta T &= \frac{\varrho}{\mathrm{d}\varrho/\mathrm{d}T}\frac{j^2}{j_{\max}^2 - j^2} \\ &= \frac{\varrho}{\alpha}\frac{j^2}{j_{\max}^2 - j^2}\end{aligned} \tag{18}$$

where $\varrho = \varrho(T)$ is the resistivity of the wire, taken at the equilibrium temperature T before switching on the current. The maximum current density $j_{\max}$ is given by

$$j_{\max} = \left(\frac{K}{t\,\mathrm{d}\varrho/\mathrm{d}T}\right)^{1/2} = \left(\frac{K}{t\,\alpha}\right)^{1/2}, \tag{19}$$

K being the contact heat conductance to the chip substrate. In terms of $j_{\max}$, the magnetic gradient becomes

$$\frac{\mathrm{d}B}{\mathrm{d}z} \approx \frac{2\mu_0}{\pi}\sqrt{\frac{K}{\alpha}}\frac{j}{j_{\max}}\frac{\sqrt{t}\,w}{w^2+4z^2}. \tag{20}$$

A typical value at a height $z = w/2$ is 10^6 G/cm for a gold wire in contact with a silicon substrate [26] ($t = 1\,\mu$m, $w = 10\,\mu$m, $j = j_{\max}$).

In the following optimization we use an expression for the trap loss rate due to thermally induced spin flips which

can be derived from reference [17] in the flat wire limit ($z, w \gg t$)

$$\gamma \approx A \frac{T_w}{\varrho(T_w)} \frac{3\pi\, t}{8z^2\,(1+(2z/w)^2)^{1/2}} \tag{21}$$

with $A = \mu_B^2 g_F^2 \mu_0^2 k_B/(2\pi\hbar)^2$. Here, $T_w = T + \Delta T$ is the actual wire temperature.

We now want to minimize γ while maintaining a fixed, large magnetic gradient $\mathrm{d}B/\mathrm{d}z$ and hence fixed transversal confinement (fixed trap oscillation frequency). Eliminating t in favor of $\mathrm{d}B/\mathrm{d}z$ in equation (21), and taking into account wire heating equation (18), we find

$$\gamma \approx A' \left(\frac{\mathrm{d}B}{\mathrm{d}z}\right)^2 \frac{(w^2+4z^2)^{3/2}}{z^2 w} \left(\frac{T}{\Delta T}+1\right) \tag{22}$$

where

$$A' = 3\pi^3 A/(32K\mu_0^2) \approx 0.8\,\mathrm{s}^{-1} \times \frac{g_F^2}{K} \tag{23}$$

where K is given in units of 10^6 W/Km^2 and the gradient $\mathrm{d}B/\mathrm{d}z$ in equation (22) in units of 10^6 G/cm. For Rb atoms ($g_F = 1/2$) and typical atom chip wires ($K \approx 5\times10^6$ W/Km^2) [26] and a magnetic field gradient of 10^5 G/cm (resulting in a trap frequency $\omega/2\pi \sim 100$ kHz) we find a typical loss rate of $\gamma \approx 4 \times 10^{-4}(T/\Delta T + 1)$ s^{-1}, or a life time > 100 s.

Both trap geometry and wire material allow to reduce this loss rate. For the geometric considerations we see that both small and large distances from the wire are unfavorable. The fraction involving the trap height z in equation (22) is minimized for $z = w/\sqrt{2}$ where the gradient is still close to its maximum value, see equation (17). This is the optimum for a fixed temperature increase of the wire, $\Delta T/T = \mathrm{const.}$

Alternatively one can work on reducing $T/\Delta T + 1$ which depends on the material properties of chip and wire and can be expressed as:

$$\frac{T}{\Delta T} + 1 = \frac{\mathrm{d}\varrho}{\mathrm{d}T}\frac{T}{\varrho}\frac{j_{\max}^2 - j^2}{j^2} + 1. \tag{24}$$

This can be minimized by choosing a current density j as close as possible to the theoretical maximum $j_{\max}$. The lowest value is then given by the '+1'. This represents Joule heating (ΔT) of the wire with a substrate held at $T = 0$.

At a fixed ratio $j/j_{\max}$, the first term involving T/ϱ is determining the temperature dependence. In this term the material properties of the wire enter. Within the linear temperature dependence for $\varrho(T)$ assumed here, it can be reduced by cooling, as shown in Figure 8 where equation (24) is plotted vs. the dimensionless temperature $\alpha T/\varrho_0$.

Two strategies are visible in this figure. Increasing the current density (compare $j/j_{\max} = 0.3$ and 0.7), allows to achieve the same gradient with a thinner wire: from equation (20), $(j/j_{\max})\sqrt{t} = \mathrm{const.}$, and the loss rate becomes smaller. In practice, the limits of this strategy are set by instabilities occurring for a close-to-critical current.

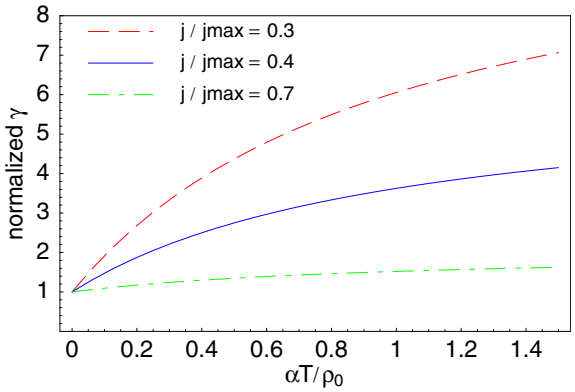

Fig. 8. Scaling of trap loss rate (22) with temperature at fixed confinement. Linear model for the resistivity, $\varrho = \varrho_0 + \alpha T$. Lines: fixed ratio to critical current density $j/j_{\max}$ [we actually plot the expression (24)]. The temperature is scaled to the dimensionless quantity $\alpha T/\varrho_0$.

At fixed $j/j_{\max}$, the loss rate can be reduced by lowering the temperature (Fig. 8). For $\alpha T \ll \varrho_0$ the loss rate γ decreases linear with T. The temperature where this linear decrease with cooling sets in ($T \ll \varrho_0/\alpha$) is higher for materials with large resistivity and small $\alpha = \mathrm{d}\varrho/\mathrm{d}T$. Materials with large ϱ_0 can be found among alloys, as suggested by Dikovsky et al. [34].

5 Summary and outlook

We have studied the lifetime of magnetically trapped atoms above a layered atom chip. Numerical calculations have been performed for the loss rate due to spin flips induced by thermal magnetic near fields, taking into account multiple reflections in the layers. Experimentally, we have been able to shift the trap center with respect to a current carrying wire, in order to differentiate between current fluctuations of technical origin, on the one hand, and intrinsic thermal noise in the chip surface, on the other. The data roughly agree with a theory without adjustable parameters. Trap loss at a large lateral distance from the wire is dominated by thermally induced spin flips. The finite thickness of the topmost layer does play a role here, and it helps to increase the trap lifetime if it is substantially thinner than the skin depth at the Larmor frequency. At shorter distance, atom-surface potentials of the van der Waals-Casimir-Polder type lower the trap barrier and open additional loss channels. In future work, the control over the trap position will permit to separate quantitatively the magnitude of technical noise sources in both the acoustic and radio frequency range. These ranges involve different mechanisms for trap loss on the microscopic level, either heating or spin flips. Optimizing the wire geometries we expect that life times >100 s can be achieved even for tight confinement with trap frequencies exceeding 100 kHz.

This work has been supported by the European Commission in the framework of the project ACQP (contract IST-2001-38863), the EU networks FASTNet (contract HPRN-CT-2002-00304) and AtomChips (contract MRTN-CT-2003-505032), and the DFG Schwerpunktprogramm: *Interactions in ultracold Atomic and Molecular gases*.

References

1. R. Folman, P. Krüger, J. Schmiedmayer, J. Denschlag, C. Henkel, Adv. Atom. Mol. Opt. Phys. **48**, 263 (2002)
2. J. Reichel, Appl. Phys. B **74**, 469 (2002)
3. T. Calarco, E.A. Hinds, D. Jaksch, J. Schmiedmayer, J.I. Cirac, P. Zoller, Phys. Rev. A **61**, 022304 (2000)
4. J. Schmiedmayer, R. Folman, T. Calarco, J. Mod. Optics, **49**, 1375 (2002)
5. Y. Wang et al., e-print `arXiv:cond-mat/0407689`
6. H. Ott, J. Fortagh, G. Schlotterbeck, A. Grossmann, C. Zimmermann, Phys. Rev. Lett. **87**, 230401 (2001)
7. W. Hänsel, P. Hommelhoff, T.W. Hänsch, J. Reichel, Nature **413**, 498 (2001)
8. A.E. Leanhardt et al., Phys. Rev. Lett. **89**, 040401 (2002)
9. S. Schneider et al., Phys. Rev. A **67**, 023612 (2003)
10. C.D.J. Sinclair et al., e-print `arXiv:cond-mat/0503619` (2005)
11. P.K. Rekdal, S. Scheel, P.L. Knight, E.A. Hinds, Phys. Rev. A. **70**, 013811 (2004); S. Scheel, P.K. Rekdal, P.L. Knight, E.A. Hinds, e-print `arXiv:quant-ph/0501149.`
12. D.M. Harber, J.M. Obrecht, E.A. Cornell, J. Low Temp. Phys. **133**, 229 (2003)
13. C. Henkel, M. Wilkens, Europhys. Lett. **47**, 414 (1999)
14. C. Henkel, S. Pötting, M. Wilkens, Appl. Phys. B **69**, 379 (1999)
15. T. Varpula, T. Poutanen, J. Appl. Phys. **55**, 4015 (1984)
16. Q.A. Turchette et al., Phys. Rev. A **61**, 063418 (2000)
17. C. Henkel, S. Pötting, Appl. Phys. B **72**, 73 (2001)
18. C. Henkel, Eur. Phys. J. D **35**, 59 (2005)
19. G.S. Agarwal, Phys. Rev. A **11**, 230 (1975)
20. P. Yeh, *Optical Waves in Layered Media* (John Wiley & Sons, New York, 1988)
21. Y.-J. Lin, I. Teper, C. Chin, V. Vuletić, Phys. Rev. Lett. **92**, 050404 (2004)
22. S. Bauer, Am. J. Phys. **60**, 257 (1992)
23. A.E. Leanhardt, Y. Shin, A.P. Chikkatur, D. Kielpinski, W. Ketterle, D.E. Pritchard, Phys. Rev. Lett. **90**, 100404 (2003)
24. J. Fortagh, H. Ott, S. Kraft, A. Günther, C. Zimmermann, Phys. Rev. A **66**, 041604(R) (2002)
25. M.P.A. Jones, C.J. Vale, D. Sahagun, B.V. Hall, E.A. Hinds, Phys. Rev. Lett. **91**, 080401 (2003)
26. S. Groth et al., Appl. Phys. Lett. **85**, 2980 (2004)
27. S. Wildermuth et al., Phys. Rev. A **69**, 030901(R) (2004)
28. E. Haller, Diploma thesis, Universität Heidelberg (2004)
29. A. Haase et al., Phys. Rev. A **64**, 043405 (2001)
30. J. Reichel, W. Hänsel, T.W. Hänsch, Phys. Rev. Lett. **83**, 3398 (1999)
31. J. Estève, Ph.D. thesis, Université Paris 6 (2004)
32. N.W. Ashcroft, N.D. Mermin, *Solid State Physics* (Saunders, Philadelphia, 1976)
33. P. Krüger, Ph.D. thesis, Universität Heidelberg (2004), `http://www.ub.uni-heidelberg.de/archiv/4905`
34. V. Dikovsky, Y. Japha, C. Henkel, R. Folman, Eur. Phys. J. D **35**, 87 (2005)